Ab initio study of the mechanism of the reaction ClO + O → Cl + O$_2$

S. Naskar, G. Nandi, T. K. Ghosh**

Department of Physics, Diamond Harbour Women's University, Sarisha, West Bengal-743368, India.

Corresponding author: T. K. Ghosh, email: tapaskrg@yahoo.com

Abstract. Ab initio investigation on the reaction mechanism of ClO + O → Cl + O$_2$ reaction has been performed using correlation consistent triple zeta basis set. The geometry and frequency of the reactants, products, minimum energy geometries and transition states are obtained using MP2 method and energetics are obtained at the QCISD(T)//MP2 level of theory. Primarily, a possible reaction mechanism is obtained on the basis on IRC calculations using MP2 level of theory. To obtain true picture of the reaction path, we performed IRC calculations using CASSCF method with a minimal basis set 6-31G**. Some new equilibrium geometries and transition states have been identified at the CASSCF level. Energetics are also obtained at the QCISD(T)//CASSCF method. Possible reaction paths have been discussed, which are new in literature. Heat of reaction is found to be consistent with the experimental data. Bond dissociation energies to various dissociation paths are also reported.
Keywords: Electronic structure; reaction mechanism; ozone depleting reaction.

Resumen. La investigación ab initio sobre el mecanismo de reacción de la reacción ClO + O → Cl + O$_2$ se ha realizado utilizando un conjunto de correlación consistente triple-zeta. La geometría y frecuencia de los reactivos, productos, geometrías de energía mínima y estados de transición se obtienen mediante el método MP2 y las energéticas se obtienen al nivel teórico QCISD(T)//MP2. En primer lugar, se obtiene un posible mecanismo de reacción sobre la base de cálculos de IRC utilizando el nivel de teoría MP2. Para obtener una imagen real de la ruta de reacción, realizamos cálculos de IRC utilizando el método CASSCF con una base mínima establecida de 6-31G**. Se han identificado algunas geometrías de equilibrio y estados de transición nuevos a nivel CASSCF. Las energéticas también se obtienen en el método QCISD(T)//CASSCF. Se han discutido posibles vías de reacción, que son nuevas en la literatura. Se encuentra que el calor de reacción es consistente con los datos experimentales. También se informan las energías de disociación de enlaces a varios caminos de disociación.
Palabras clave: Estructura electrónica, mecanismo de reacción, agotamiento de la capa de ozono.

Introduction

Recently, a worldwide concern has been grown up about the environmental threat on the earth due to the depletion of ozone layer in the atmosphere, particularly in the lower stratosphere. The halogen atoms and their oxides play a key role in atmospheric ozone destruction. One of the important catalytic ozone depleting cycles is:

$$ClO + O \rightarrow Cl + O_2 \tag{1}$$

$$Cl + O_3 \rightarrow ClO + O_2, (\text{Net: } O + O_3 \rightarrow 2O_2) \tag{2}$$

The reaction (1) is the rate-limiting step in this catalytic cycle and so this reaction is crucial for determining the efficiency of ozone depletion and its trends. The depletion of ozone by Cl atoms was first reported by Molina and Rowland [1]. Importance of chlorine oxides in atmospheric ozone destruction was described by Stolarski and Cicerone [2]. The kinetics of the reaction of ClO with O was studied experimentally over a temperature range using discharge flow resonance technique by Schwab et al. [3], Ongstad and Birks [4], Goldfrab et al. [5], etc. The reaction of ClO with O proceeds via the isomers ClO_2. Two isomeric structures are possible: symmetric (C_{2v}) chlorine dioxide OClO and asymmetric (C_s) chlorine peroxide ClOO. The OClO isomer is stable at room temperature, whereas ClOO rapidly dissociates to Cl and O_2. The OClO and ClOO radicals were studied by several experimentalists, eg. matrix isolation study by Arkell and Schwager [6], Gole [7] and Johnsson et al. [8], microwave spectra analysis by Miyazaki et al. [9], IR spectra analysis by Muller and Willner [10]. Among the theoretical investigations, structure, bonding properties and thermochemistry of $ClO2$ radical were studied by Francisco and Sander [11], Beltran et al. [12] and Li et al [13]. Multiconfiguration CI calculations were reported by Peterson and Werner [14] on the first four doublet states (X^2B_1, $^2B_2$, $^2A_1$, A^2A_2) of OClO and X^2A'' of ClOO for their geometry, frequency, dissociation energy, etc. They suggested qualitatively that OClO predissociates to ClO + O_2 via the excited state as OClO (X^2B_1) + hv $\rightarrow$ OClO (1^2A_2)$\rightarrow$ClO + O_2. A direct dissociation is also reported to be possible as ClO+$O_2$$\rightarrow$ClOO ($X2A''$)$\rightarrow$ClO+$O_2$. The only ab initio investigation on the reaction mechanism and kinetics of this reaction was reported by Zhu and Lin [15]. They reported two transition states which are more than 61 kcal/mol above the equilibrium geometries OClO and ClOO and so the product formation happens directly via the equilibrium geometry ClOO.

In the present article, ab initio calculations have been done to investigate various minimum energy geometries, transition state geometries, heat of reactions and possible reaction pathways of the ozone depleting reaction (1), viz. ClO + O $\rightarrow$ Cl + O_2. The bond dissociation energies of the OClO and ClOO isomers have also been obtained. In the following sections, we have discussed the computational methodology used followed by results and discussion.

Method and computational details

We consider the ground state potential energy surface of the reaction ClO(2Π) + O($3P$) $\rightarrow$ Cl($2P$) + O_2($3\Sigma g$-). We employed cc-pVTZ basis set for oxygen and chlorine atoms [16] and added a set of s and p diffuse functions of exponents 0.07376, 0.05974 for O, 0.0591, 0.0419 for Cl, respectively from augmented sets [16]. The d and f diffuse functions are not taken into the calculations to minimize the computational cost. All the reactants, products, minimum energy geometries and transition states are optimized at the second order Moller-Plesset perturbation theory (MP2). The vibrational frequencies are also obtained at the MP2 level. Primarily, to track out a possible reaction path, internal reaction coordinate (IRC) calculations have been performed at the MP2 level using step sizes 0.2-0.5 amu1/2.bohr for various cases along the reaction path. Since the bonds are broken and formed along the reaction path, a single configuration approach, like the present MP2 method, may not provide the true picture of the reaction path. So, in addition, we performed IRC calculations using CASSCF(7,6) method with step size 0.2-0.5 amu1/2.bohr, where we have chosen 7 electrons in 6 active space and 6-31G** basis set to reduce the computational cost. Several equilibrium geometries and transition states are optimized at the CASSCF(7,6) method. It is to be noted at this point that geometries obtained at the CASSCF(7,6)/6-31G** method may not be very close to the available data. Our aim of the CASSCF calculations is to find out the true picture of the reaction path of the said reaction. Single point energy (E) calculations are performed using quadratic configuration interaction with single-double including triples substitutions QCISD(T) method at the MP2 optimized geometries obtained using the first sets of triple-zeta basis, as well as using QCISDT(T) method at the CASSCF(7,6) optimized geometries using the 6-31G** basis set. The relative energy (ΔE) of the various isomers is the then obtained with respect to reactants at the MP2, QCISD(T)//MP2 methods and CASSCF, QCISD(T)//CASSCF methods. The enthalpy correction ($\Delta H298$) and Gibbs energy correction ($\Delta G298$) at298.15 K obtained at the MP2 and CASSCF levels are noted down to obtain

relative enthalpy () and relative Gibbs energy () with respect to reactants at the MP2, QCISD(T)//MP2 and CASSCF, QCISD(T)//CASSCF methods. The tabulated experimental heat of reactions ($\Delta rH298$) are obtained using the experimental heat of formations of O (59.55 ± 0.01), Cl (28.99), O2 (0), ClO (24.29±0.03), in kcal/mol, from NIST-JANAF compilations [17]. It is to be noted that the experimental spin orbit corrections (SOC) of Cl (-0.84 kcal/mol), and ClO (-0.45 kcal/mol) [18] are of minor importance for the present systems under investigation. All the calculations are performed using Gaussian 03W program system [19]. *socH298ΔsocG298Δ*

Results and discussion

Structure and energetics

In Table 1, we have listed our optimized geometry and vibrational frequency of the reactants, products, equilibrium geometries and transition states both at the MP2 and CASSCF methods along with the available data for comparison. It is found that the maximum deviation in our calculated bond lengths for reactants and products at the MP2 level is about 0.02 Å compared to experimental values [20]. At the MP2 level, we obtained three equilibrium geometry EG1-OClO (X^2B_1) in C_{2v} symmetry, EG2-ClOO ($2^2A''$) in Cs symmetry (corresponding to $^2A_2$ state in C_{2v} symmetry [7]) and EG3-ClOO (X^2A'') in C_s symmetry. The geometry of EG1 and EG3 obtained at the MP2 level are found in good agreement with the available experimental data. The equilibrium geometry EG1-OClO ($^2B_1$) obtained at the CASSCF level is an excited state of same $^2B_1$ symmetry, which is reflected from the energy value listed in Table 2. At the CASSCF level, we find a larger Cl-O distance and ClOO angle for EG3 as compared to those at MP2 level. The Mulliken charge analysis of EG3 at the both methods show that it is of Cl.OO type. Reported equilibrium geometries of Zhu and Lin [15] are compared with our geometries EG1 and EG3. We obtained a new geometry EG2-ClOO ($2^2A''$), which is the 1st excited state of EG3. At the CASSCF level, we obtained two more equilibrium geometries EG4-ClOO ($1^2A'$) and its excited member EG5-ClOO ($2^2A'$). The Cl-O distance in EG4 becomes large enough to 3.6680 Å. It has the OO distance 1.2425 Å, whereas EG3 has OO distance of 1.1890 Å, which is very close to the equilibrium bond length of O_2, viz. 1.1901 Å at the CASSCF level. The Mulliken population analysis of EG3 predicts that it is of Cl.O_2 type (mentioned later in IRC results) and so possibly responsible for product formation. From Table 2 we see that, EG4-ClOO($1^2A'$) lies below EG3-ClOO ($1^2A''$) by 0.42 kcal/mol (relative Gibbs energy at the QCISD(T)//CASSCF level). In actual situation, $1^2A'$ state (ie. EG4) should lie above $1^2A''$ state (ie. EG3). A higher correlated method or more extensive basis set is expected to remove this discrepancy.

We obtained three transition states TS1-OClO ($^2B_2$), TS2-ClOO ($^2A'$) and TS3-ClOO ($^2A''$), at the MP2 level. Zhu and Lin [15] reported two transition states, which are tentatively compared with our TS1 and TS2, respectively. It is to be noted that they did not mention the state of these transition structures. The geometry of TS1 and TS2 are very similar and their MP2 and QCISD(T)//MP2 energies are found almost same (Table 2). TS1 and TS2 are the transition states belonging to C_{2v} and C_s symmetries, respectively. A difference of 0.15 kcal/mol is reflected in their relative Gibbs energy values, which is due to the differences in their frequency values. At the QCISD(T)//CASSCF level this difference comes out to be 1.25 kcal/mol as compared to 1.8 kcal/mol of Zhu and Lin [15]. The transition state TS3-ClOO ($1^2A''$) is found to be a new one. The bond distances and bond angle are slightly larger at the CASSCF level as compared to MP2 level. Both the methods depicts that this TS3 is of the Cl-OO type supported by their Mulliken charge populations. It is to be noted that both the methods offer a large spin contamination error ($<S^2>=1.25$-1.78) for EG3, EG4 and TS3. The transition state TS4-ClOO ($2^2A''$) is an excited member of TS3-ClOO ($1^2A''$) obtained at the CASSCF level and it is basically of ClO.O type. It is to be mentioned at this point that, in Table 1, the frequency values of the OClO isomers are tabulated in the sequence of bending, symmetric stretching and asymmetric stretching modes, whereas for ClOO isomers there are tabulated in the sequence of ClO stretching, bending and OO stretching modes. The transition states are verified with having one imaginary frequency.

Table 1. Optimized geometry and frequency of the isomers for the reaction ClO+O →Cl+O$_2$.

Species	Method	Geometry(Å, deg)			Frequency (cm^{-1})		
		Our calc	Expt.	Others calc	Our calc	Expt.	Others calc
ClO ($^2\Pi$)	MP2 CAS	1.5678 1.6220	1.5696[a]	1.5683[b]	849.4 982.9	853.8[a]	856.7[b]
O$_2$ ($^3\Sigma$g$^-$)	MP2 CAS	1.2233 1.1901	1.207[a]	1.2095[c]	1462.5 1826.0	1580.2[a]	1585[c]
EG1-OClO (X^{2}B$_1$) C$_{2v}$ EG1-OClO (^{2}B$_1$)C$_{2v}$	MP2 CAS	1.4891, 117.7 1.5120, 121.0 (R13=2.6320)	1.4698, 117.4[d]	1.4960, 117.9[g]	443.3,1007.6, 1168.8 426.3,877.8, 1140.3	448.7, 944.8, 1107.6[e]	443, 924, 1070[g]
EG2-ClOO (2^{2}A") C$_s$	MP2 CAS	1.7157,1.2655, 113.2 1.8101,1.3228, 109.8			500.5,1104.1, 1643.1 364.9,580.1, 1016.6		
EG3-ClOO (1^{2}A") C$_s$	MP2 CAS	2.1403,1.1590, 118.2 3.3991,1.1890, 122.2	1.831, 1.231 110[f]	1.991,1.218, 116.6[g]	218.5,477.2, 1899.8 27.8, 235.9, 1806.9	373, 407, 1441[f]	297, 516, 1417[g]
EG4-ClOO (1^{2}A')C$_s$ /OClO(^{2}B$_2$)C$_{2v}$	CAS	3.6680, 1.2425, 80.3 (A213=19.5)			34.5, 530.3, 1435.4		
EG5-ClO$_1$O$_2$ (2^{2}A')C$_s$	CAS	1.7698,1.4701, 103.0 R(ClO$_2$)=2.5417 A(ClO$_2$O$_1$)=42.7			325.2, 591.2, 716.4		
TS1-OClO (^{2}B$_2$) C$_{2v}$	MP2 CAS	1.7007, 52.8 (R13=1.5121) 2.0343, 41.9 (R13=1.4548)		1.823, 48.8[g] (R13=1.506)	-124.2, 799.4,1064.6 -6694.6, 537.7, 976.2		
TS2-ClOO (^{2}A')C$_s$	MP2 CAS	1.7032,1.5133, 63.4 (R13=1.6983) 2.0909,1.5460, 68.3		1.908, 1.593, 62.7[g]	-597.7, 852.5,1187.0 -1920.2, 265.0,721.9		
TS3-ClOO (1^{2}A") C$_s$	MP2 CAS	1.8377, 1.2011, 115.5 2.2243,1.2338, 112.8			-1038.0, 505.4, 1454.6 -283.0, 343.6,1059.0		
TS4-ClOO (2^{2}A") C$_s$	CAS	1.6277,2.2133, 105.9			-96.3, 159.7, 860.5		

[a]Reference [20]; [b]Reference [21]; [c]Reference [22]; [d]Reference [9]; [e]Reference [10]; [f]Reference [6]; [g]Reference [15] (PW91PW91/6-3111G(3df)).

Table 2. Relative energy of the isomers for the reaction ClO + O →Cl + O$_2$.

Species	Method	Electronic energy E (au)	Relative energy w.r.to reactants ΔE (kcal/mol)	Enthalpy correction ΔH$_{298}$ (kcal/mol)	Relative enthalpy w.r.to reactants ΔH_{298}^{corr} (kcal/mol)	Gibbs energy correction ΔG$_{298}$ (kcal/mol)	Relative Gibbs eng w.r.to reactants ΔG_{298}^{corr} (kcal/mol)	Expt. value[a] (kcal/mol)	Others calc[b] kcal/mol)

Reactants:ClO + O	MP2
	QCISD(T)//MP2
	CAS
	QCISD(T)//CAS
		-609.646391
		-609.713718
		-609.005695
		-609.440137
			0.00
			0.00
			0.00
			0.00
				3.33
				
				3.50
					0.00
					0.00
					0.00
					0.00
						-12.41
						
						-12.25
							0.00
							0.00
							0.00
							0.00
								0.00	0.00

EG1-OClO (X^{2}B$_1$)
EG1-OClO (^{2}B$_1$)
	MP2
	QCISD(T)//MP2
	CAS
	QCISD(T)//CAS
		-609.753053
		-609.789646
		-609.009406
		-609.486398
			-66.93
			-47.64
			-2.33
			-29.03
				6.32
				
				6.09
					-63.94
					-44.65
					0.26
					-26.44
						-11.98
						
						-12.25
							-66.50
							-47.21
							-2.33
							-29.03
								-60.66±1.95
								
								--
									-58.0
									
									--

EG2-ClOO
(2^{2}A")
	MP2
	QCISD(T)//MP2
	CAS
	QCISD(T)//CAS
		-609.735026
		-609.796603
		-609.095216
		-609.520283
			-55.62
			-52.01
			-56.17
			-50.29
				7.17
				
				5.52
					-51.78
					-48.17
					-54.15
					-48.27
						-11.57
						
						-13.60
							-54.78
							-51.17
							-57.52
							-51.64		

EG3-ClOO
(1^{2}A")
	MP2
	QCISD(T)//MP2
	CAS
	QCISD(T)//CAS
		-609.743371
		-609.802053
		-609.093184
		-609.531065
			-60.85
			-55.43
			-54.90
			-57.06
				6.57
				
				5.54
					-57.61
					-52.19
					-52.86
					-55.02
						-12.90
						
						-15.46
							-61.34
							-55.92
							-58.11
							-60.27
								-60.42±1.00	-60.4

EG4-ClOO (1^{2}A')	CAS QCISD(T)//CAS	-609.102817 -609.532751	-60.94 -58.12	5.90	-58.54 -55.72	-14.82	-63.51 -60.69		
EG5-ClOO (2^{2}A')	CAS QCISD(T)//CAS	-609.065461 -609.472073	-37.50 -20.04	5.12	-35.88 -18.42	-14.17	-39.42 -21.96		

TS1-OClO
(^{2}B$_2$)
	MP2
	QCISD(T)//MP2
	CAS
	QCISD(T)//CAS
		-609.642497
		-609.697237
		-608.971704
		-609.420284
			2.44
			10.34
			21.33
			12.46
				5.10
				
				4.68
					4.21
					12.11
					25.51
					13.64
						-13.07
						
						-13.80
							1.78
							9.68
							19.78
							10.91
									5.3

TS2-ClOO
(^{2}A')
	MP2
	QCISD(T)//MP2
	CAS
	QCISD(T)//CAS
		-609.642498
		-609.697240
		-609.011816
		-609.420060
			2.44
			10.34
			-3.84
			12.60
				5.34
				
				4.14
					4.45
					12.35
					-3.20
					13.24
						-13.22
						
						-15.19
							1.63
							9.53
							-6.78
							9.66
									3.5

TS3-ClOO (1²A")	MP2	-609.722746	-47.91	5.31	-45.93	-13.43	-48.93		
	QCISD(T)//MP2	-609.798410	-53.14		-51.16		-54.16		
	CAS	-609.088507	-51.96	4.62	-50.84	-14.52	-54.23		
	QCISD(T)//CAS	-609.528589	-55.50		-54.38		-57.77		
TS4-ClOO (2²A")	CAS	-609.012981	-4.57	4.26	-3.81	-15.51	-7.83		
	QCISD(T)//CAS	-609.433205	4.35		5.11		1.09		
Products: Cl+ O_2	MP2	-609.756865	-69.32	4.17	-68.48	-10.45	-67.36	-54.85±0.04	-55.8
	QCISD(T)//MP2	-609.805189	-57.40		-56.56		-55.44		
	CAS	-609.113736	-67.80	4.68	-66.62	-9.90	-65.45		
	QCISD(T)//CAS	-609.530364	-56.62		-55.44		-54.27		

[a]Reference [17] (using expt. heat of formations); [b]Reference [15] (G2M//PW91PW91/6-3111G($3df$)).

The relative energies of the various geometries with respect to reactants are listed in Table 2. The relative enthalpy and the relative Gibbs energy w.r.to reactants at the MP2 and CASSCF methods are also listed in the table for a comparative study. Our calculated EG1 at the QCISD(T)//MP2 level is found to be over estimated by only 6 kcal/mol compared to the experimental value obtained using experimental heat of formations. An overestimation of 8 kcal/mol has been found as compared to the only available theoretical value of Zhu and Lin [15], which is the relative energy obtained at the G2M//PW91PW91/6-3111G(3df) level. A large deviation has been occurred between CASSCF and QCISD(T)//CASSCF results for EG1. For EG2, both the QCISD(T)//MP2 and QCISD(T)//CASSCF methods predict almost equal energy values. A similar feature has been observed for EG3. The relative Gibbs energy for EG3 obtained at the QCISD(T)//CASSCF level is in very good agreement with the experimental data. As mentioned earlier, EG4 is found below EG3, which may be due to smaller basis set or methodology used. EG5 is the excited state of EG4 which is reflected from its relative energy value. We found for most of the transition states, the relative Gibbs energies are increased at the QCISD(T)//CASSCF level compared to QCISD(T)//MP2 level. As mentioned earlier, TS1 is 1.25 kcal/mol above TS2 at the QCISDT)//CASSCF level, as compared to predicted value of 1.8 kcal/mol by Zhu and Lin [15]. The relative enthalpy of the products w.r.to reactants (), which is the heat of reaction (*corrH*298$\Delta\Delta$r*H*298), is found to be -56.56 kcal/mol at the QCISD(T)//MP2 level and -55.44 kcal/mol at the QCISD(T)// CASSCF level, which are found in good agreement with the experimental value of -54.85±0.04 kcal/mol [17]. If we include spin orbit corrections of Cl and ClO [18], they becomes -56.95 and -55.83 kcal/mol, respectively.

The IRC result of TS1-OClO (X^2B_2) along the minimum energy path using MP2 method is depicted in Fig. 1. MP2 and CASSCF energies of all the geometries are also listed in Table 2, which may be helpful for understanding the IRC results. Fig. 1 shows that TS1 represents the energy barrier for the process EG1-OClO ($^2B_1$)→Cl+O_2. The OCl distance increases gradually from EG1→TS1→Products as:1.4891→1.7007→3.6586 Å and OO distance converges to equilibrium bond length of O_2 as 2.28→1.51→1.2281 Å. So, the possible reaction path is: ClO+O→EG1-OClO(X^2B_1)→TS1-OClO ($^2B_2$)→Cl+O_2. But this path is unlikely to be observed as TS1 is at large barrier height of 56.89 kcal/mol (Gibbs energy difference at QCISD(T)//MP2 level) above EG1.
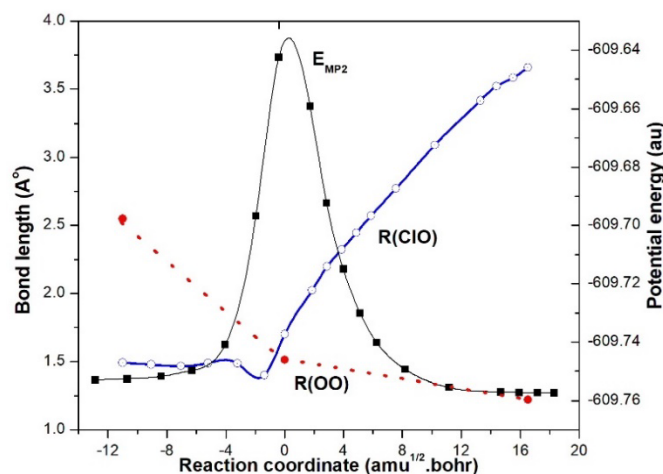

Fig. 1. IRC/MP2 result of TS1: EG1-OClO(X^2B_1)-TS1-OClO($^2B_2$)-Cl + O_2.

We performed IRC calculation for TS2. Along the reverse direction it connects to EG2-ClOO ($2^2A''$), but along the forward direction it fails to predict any equilibrium geometry and that's why, it is not shown here. Also TS2 has a large barrier height 60.70 kcal/mol above EG2 and so this path is also unlikely to be followed. The ground state of Cl atom (^2P) and excited state of O2 ($^1\Delta g$) can be combined to yield 2A'' and 2A' states. So this TS2-ClOO ($^2A'$) may be responsible for the dissociation to the excited state Cl+O2 ($^1\Delta g$). Such a correlation diagram for the equilibrium geometries was mentioned by Gole [7].

The TS3-ClOO (1^2A") is the transition state for the isomerisation process EG2-ClOO (2^2A")→EG3-ClOO (1^2A"), which is clear from the gradual changes of ClO and OO bond lengths on both sides of the transition state, as shown in Fig. 2. Note that there is a gradual increase of ClO distance as 1.7157→1.8377→2.1403 Å and a gradual decrease of OO distance as 1.2655→1.2011→1.1590 Å along the path EG2-ClOO (2^2A")→TS3-ClOO (1^2A")→EG3-ClOO (1^2A"). It is to be noted from the relative Gibbs energy in Table 2, that TS3 lies above EG2 at the MP2 level, but at the QCISD(T) level it moves below EG2. Such energy reordering is probably due to the methodology used.
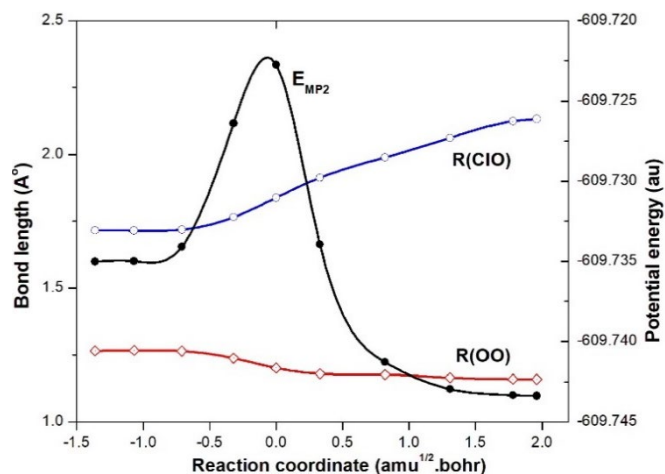
Fig. 2. IRC/MP2 result of TS3: EG2-ClOO(2^2A") -TS3-ClOO(1^2A")- EG3-ClOO(1^2A").

The possible reaction path for the product formation, as obtained by IRC/MP2 method is shown on the LHS in Fig. 3, which are: ClO+O→EG2-ClOO(2^2A")→TS3-ClOO(1^2A")→EG3-ClOO(1^2A")→Cl+O$_2$. A direct reaction process ClO+O→EG3-ClOO(1^2A")→Cl+O$_2$ is also possible if we omit TS3 because of its large spin contamination. The second path was mentioned by Zhu and Lin [15]. The first reaction path reported here is associated with the identification of new geometries EG2 and TS3 and also supported by IRC calculation. In Fig. 3, the relative Gibbs energy of the geometries w.r.to reactants are shown at the MP2 and QCISD(T)//MP2 (within parenthesis) levels. The detail values of the structures given in Fig. 3 are now shown because of space problem, however they can be found out in Table 1.
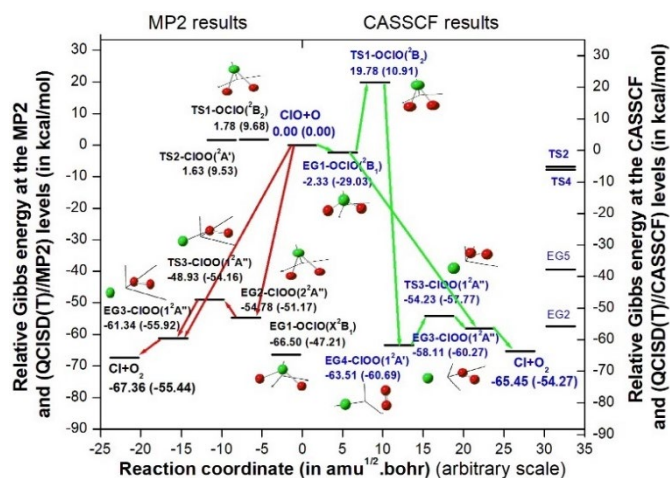

Fig. 3. Relative Gibbs energy w.r.to reactants and reaction pathways.

The IRC result of TS2-ClO$_1$O$_2$ (^{2}A') at the CASSCF level is shown in Fig. 4. The variation of bond distances ClO$_1$, ClO$_2$ and O$_1$O$_2$ as well as CASSCF energy clearly depicts the interchanges of O atoms in EG5 as EG5-ClO$_1$O$_2$ (2^2A') to EG5-ClO2O1 (2^2A') along the reaction path. The IRC result of TS4-ClO$_1$O$_2$ (2^2A") is shown in Fig. 5, which is also shown to be confined to the geometry EG2-ClOO (2^2A") on both sides of the reaction path. Since TS2 and TS4 are not contributing anything to the reaction mechanism, only their relative positions are shown on the RHS in Fig. 3.
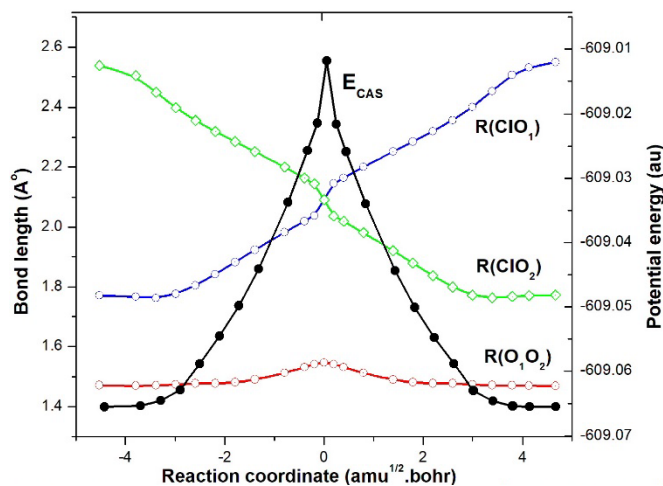
Fig.4. IRC/CAS result of TS2: EG5-ClO$_1$O$_2$(2^2A') – TS2-ClO$_1$O$_2$(^{2}A') - EG5-ClO$_2$O$_1$(2^2A').
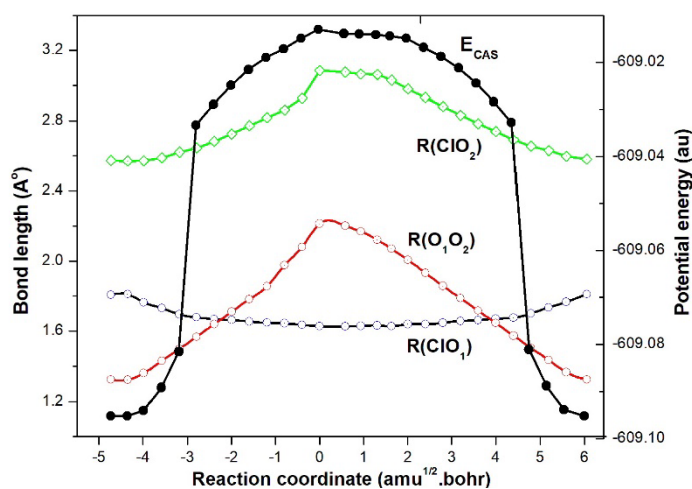
Fig. 5. IRC/CAS result of TS4: EG2-ClOO(2^2A") - TS4-ClOO(2^2A") - EG2-ClOO(2^2A").

The IRC result of TS1-OClO (2B2) along the minimum energy path using CASSCF method is depicted in Fig. 6. It shows that TS1 represents the energy barrier for the process EG1-OClO (^{2}B1)→EG4-ClOO (1^{2}A'). The bond distance ClO increases gradually from EG1→TS1→EG4 as: 1.5120→2.0343→3.6680 Å and OO distance decrease as 2.6320→1.4548→1.2425 Å. So a part of the reaction path is: ClO+O□EG1-OClO(^{2}B$_1$)→TS1-OClO(^{2}B$_2$)→EG4-ClOO (1^{2}A').
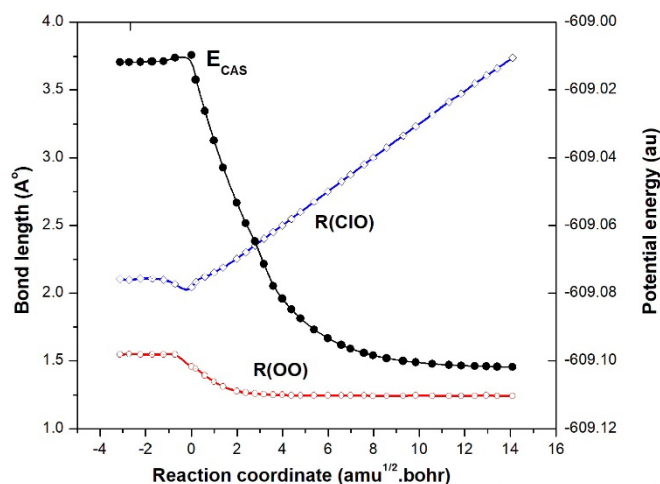
Fig. 6. IRC/CAS result of TS1: EG1-OClO ($^2B_1$) - TS1-OClO ($^2B_2$) - EG4-OClO($1^2A'$).

The result of IRC calculation at the CASSCF level for TS3-ClOO ($1^2A''$) is shown in Fig. 7. It represents the isomerisation process from EG4-ClOO ($1^2A'$) to EG3-ClOO ($1^2A''$), which is clear from the gradual changes of ClO and OO bond lengths on both sides of the transition state, as shown in the figure. Along the path EG4-ClOO ($1^2A'$)→EG3-ClOO ($1^2A''$) via TS3, there is a gradual decrease of ClO distance as 3.6680→2.2243→2.1403Å. But along this path the OO distance converges to the equilibrium bond length of O_2 as 1.2425→1.2338→1.1890 Å (R_e of O2=1.1901). The Mulliken charge population of TS3 and EG3 are (Cl: 0.001, O: 0.039, O: -0.04) and (Cl: 0.00, O: 0.01, O: -0.01), respectively. These clearly support the formation of products EG3→Cl+O_2. So, the final possible reaction path is ClO+O→EG1-OClO($^2B_1$)→TS1-OClO($^2B_2$)→EG4-ClOO($1^2A'$)→TS3-ClOO($1^2A''$)→EG3-ClOO ($1^2A''$)→Cl+O_2. A direct reaction path is also possible as ClO+O→EG3-ClOO($1^2A''$)→Cl+O_2, which was also observed at the IRC/MP2 level, as well as suggested by Zhu and Lin [15]. The possible reaction paths are shown on the RHS in Fig. 3. The relative Gibbs energy of various geometries are shown as obtained at the CASSCF and QCISD(T)//CASSCF (within parenthesis) levels.
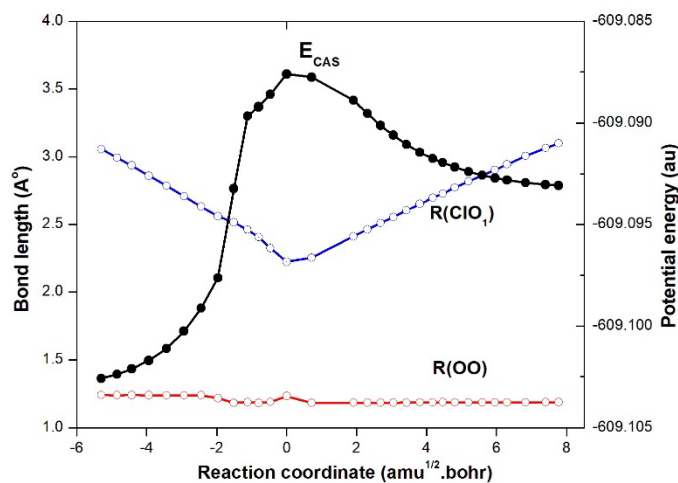

Fig.7. IRC/CAS result of TS3: EG4-ClOO($1^2A'$) - TS3-ClOO($1^2A''$) – EG3-ClOO($1^2A''$).

Bond dissociation energy

Several bond dissociation energies of the ground state dissociation of OClO (X^2B_1) and ClOO ($1^2A''$) are determined from the energy difference of the following reactions: OClO / ClOO$\rightarrow$Cl+O_2, $\rightarrow$ClO+O and $\rightarrow$Cl +2O. We used QCISD(T)//MP2 energy including MP2-ZPE correction. Our calculated values for the dissociation to Cl+O_2 for both the OClO and ClOO are found to be in good agreement with the experimental values, obtained using experimental heat of formations [17]. The BDE for the dissociation to other paths are underestimated by 6-25 kcal/mol compared to the experimental values. Higher correlated method and using more extensive basis sets may reduce this deviation.

Table 3. Bond dissociation energy of the isomers to several ground state dissociations.

Dissociation Paths	Our BDE (kcal/mol)	Expt.value[a] (kcal/mol)	Others calc[b] (kcal/mol)
OClO(X^2B_1) $\rightarrow$Cl + O_2	-11.41	-5.81±3.00	
$\rightarrow$ClO + O	45.11	60.66±1.95	60.4
$\rightarrow$ Cl + 2O	100.51	124.91±1.93	
ClOO($1^2A''$)$\rightarrow$ Cl + O_2	-3.59	-5.57±0.96	-3.9
$\rightarrow$ClO + O	52.93	60.42±1.00	59.2
$\rightarrow$ Cl + 2O	108.33	124.67±0.98	

[a]Reference [17] (Using expt. heat of formations); [b]Reference [23] (CCSD(T)/CBS).

Conclusion

We performed ab initio investigation on the reaction mechanism of ClO+O$\rightarrow$Cl+O_2 reaction, which has a potential importance in stratospheric ozone depletion. Several minimum energy geometries and transition states are identified along with some new isomers reported as first time in literature. Primarily, to track out the reaction path we performed IRC calculations at the MP2 level. For the validation and to obtain the true picture of the reaction path, we further performed IRC calculations using the CASSCF method. At the CASSCF level we explored some new equilibrium geometries and transition states. Possible reaction mechanisms have been obtained using both the methods, which are found to be new in literature. Bond dissociation energies of the isomers to several ground state dissociation asymptotes are reported.

Acknowledgments

References

1. Molina, M. J.; Rowland, F. S. *Nature.* **1974**, *249,* 810-812. DOI: https://doi.org/10.1038/249810a0
2. Stolarski, R. S.; Cicerone, R. J. *Can J. Chem*. **1974**, *52*, 1610-1615. DOI: https://dx.doi.org/10.1139/v74-233

3. Schwab, J. J.; Toohey, D. W.; Brune, W. H.; Anderson, J. G. *J. Geophys. Res.* **1984**, *89*, 9581-9587. DOI: https://dx.doi.org/10.1029/JD089iD06p09581

4. Ongstad, A. P.; Birks, J. W. *J. Chem. Phys.* **1986**, *85*, 3359-3368. DOI: https://dx.doi.org/10.1063/1.450957

5. Goldfarb, L.; Burkholder, J. B.; Ravishankara, A. R. *J. Phys. Chem. A.* **2001**, *105*, 5402-5409. DOI: https://dx.doi.org/10.1021/jp0100351

6. Arkell, A.; Schwager, I. *J. Am. Chem. Soc.* **1967**, *89*, 5999-6006. DOI: https://dx.doi.org/10.1021/ja01000a001

7. Gole, J. L. *J. Phys. Chem.* **1980**, *84*, 1333-1340. DOI: https://dx.doi.org/10.1021/j100448a009

8. Johnsson, K.; Engdahl, A.; and Nelander, B. *J. Phys. Chem*. **1993**, *97*, 9603-9606. DOI: https://dx.doi.org/10.1021/j100140a013

9. Miyazaki, K.; Tanoura, M.; Tanaka, K.,; Tanaka, T. *J. Mol. Spectrosc*. **1986**, *116*, 435-449. DOI: https://dx.doi.org/10.1016/0022-2852(86)90138-4

10. Muller, H. S. P.; Willner, H. *J. Phys. Chem.* **1993**, *97*, 10589-10598. DOI: https://dx.doi.org/10.1021/j100143a013.

11. Francisco, J. S.; Sander, S. P. *J. Chem. Phys.* **1993**, *99*, 2897-2901. DOI: https://dx.doi.org/10.1063/1.465197

12. Beltrán, A.; Andrés, J.; Noury, S.; Silvi, B. *J. Phys. Chem. A.* **1999**, *103*, 3078-3088. DOI: https://dx.doi.org/10.1021/jp983999

13. Li, Q. -S.; Lu, S.-F.; Xu, W.-G.; Xie, Y.; Schaefer III, H. F. *J. Phys. Chem. A* **2002**, *106*, 12324-12330. DOI: https://dx.doi.org/10.1021/jp020362o

14. Peterson, K. A.; Werner, H. J. *J. Chem. Phys.* **1992**, *96*, 8948-8961. DOI: https://dx.doi.org/10.1063/1.462253

15. Zhu.; R. S.; Lin, M. C. *J. Chem. Phys.* **2003**, *119*, 2075-2082. DOI: https://dx.doi.org/10.1063/1.1585027

16. Basis set exchange for Quantum Chemistry: https://www.basissetexchange.org; Dunning Jr.,T.H.*J. Chem. Phys*. **1989**, *90*, 1007-1023. DOI: https://dx.doi.org/10.1063/1.456153; Woon, D. E.; Dunning Jr., T.H. *J. Chem. Phys.***1993**, 98, 1358-1371. DOI: https://dx.doi.org/10.1063/1.46430

17. Chase, M. W. *J. Phys. Chem. Ref. Data*, Monograph No.9, NIST-JANAF Thermochemical Tables, 4th ed. 1998.

18. C. E. Moore, *Atomic Energy Levels*, NSRDS-NBS 35, Vol. 1, 3, Washington, DC, 1971.

19. Frisch, M. J.; et al., Gaussian 03W, Gaussian, Inc., Wallingbond, CT, 2003.

20. Huber, K. P.; Herzberg, G. *Molecular Spectra and Molecular Structure: Constants of Diatomic Molecules*, Vol. IV, Van Nostrand, New York, 1979.

21. Peterson, K. A.; Shepler, B. C.; Figgen, D.; Stoll, H. *J. Phys. Chem. A.* **2006**, *110*, 13877-13883. DOI: https://dx.doi.org/10.1021/jp065887l

22. Hassanzadeh, P.; Irikura, K. K.; Johnson III, R. D. *J. Phys. Chem. A.* **1997**, *101*, 6897-6902. DOI: https://dx.doi.org/10.1021/jp971007e

23. Grant, D. J.; Garner III, E. B.; Matus, M. H.; Nguyen, M. T.; Peterson, K. A.; Francisco, J. S.; Dixon, D. A. *J. Phys. Chem. A* **2010**, *114*, 4254–4265. DOI: https://dx.doi.org/10.1021/jp911320p